Süleyman Demirel Üniversitesi
Fen Bilimleri Enstitüsü Dergisi
Cilt 23, Sayı 3, 727-737, 2019

Süleyman Demirel University
Journal of Natural and Applied Sciences
Volume 23, Issue 3, 727-737, 2019

DOI: 10.19113/sdufenbed.527602

The Effect of Synthesis Conditions on Calcium Silicate Bioceramic Materials

Yasin ARSLAN[1], Erdal KENDÜZLER[2], Vahide Tuğçe ADIGÜZEL[3], Fatma TOMUL*[4]

[1]Burdur Mehmet Akif Ersoy University, Faculty of Arts and Science, Department of Nanoscience and Nanotechnology, 15100, Burdur, Turkey
[2,3,4]Burdur Mehmet Akif Ersoy University, Faculty of Arts and Science, Department of Chemistry, 15100, Burdur, Turkey

(Alınış / Received: 15.02.2019, Kabul / Accepted: 04.10.2019, Online Yayınlanma / Published Online: 30.12.2019)

Keywords
Calcium silicate bioceramic,
Materials,
Hydrothermal synthesis,
Calcination,
X-ray diffraction

Abstract: In this study, calcium silicate bioceramic materials of various Ca/Si ratios were prepared using tetraethyl orthosilicate and calcium nitrate by a hydrothermal synthesis method, taking into consideration cost-effective and environmentally friendly, 'green', synthesis rules. For comparison purposes, sol-gel synthesis method was also used. Calcium silicate bioceramic materials produced by both methods were calcined at 600°C and 950°C. Fourier Transform Infrared Spectroscopy, Thermogravimetric Thermal Analysis, Field Emission Scanning Electron Microscopy and X-ray Diffraction methods were used to characterize calcium silicate bioceramic materials. The characterization results validated the formation of calcium silicate materials.

Sentez Koşullarının Kalsiyum Silikat Biyoseramik Malzemelere Etkisi

Anahtar Kelimeler
Kalsiyum silikat biyoseramik,
Malzemeler,
Hidrotermal sentez,
Kalsinasyon,
X ışını kırınımı

Özet: Bu çalışmada, çeşitli Ca/Si oranlarındaki kalsiyum silikat biyoseramik malzemeleri, düşük maliyetli ve çevre dostu "yeşil" sentez kuralları göz önünde bulundurularak, bir hidrotermal sentez yöntemi ile hazırlanmıştır. Karşılaştırma amacıyla sol-gel sentez metodu da kullanılmıştır. Başlangıç materyali olarak tetraetil ortosilikat ve kalsiyum nitrat kullanılmıştır. Her iki yöntemle üretilen kalsiyum silikat biyoseramik malzemeleri 600 °C ve 950 °C'de kalsine edilmiştir. Fourier Dönüşümü Kızılötesi Spektroskopisi, Termogravimetrik Termal Analiz, Alan Emisyon Taramalı Elektron Mikroskobu ve X-Işını Kırınımı metodları kalsiyum silikat biyoseramik malzemeleri karakterize etmek için kullanılmıştır. Karakterizasyon sonuçları kalsiyum silikat malzemelerinin oluşumunu doğrulamıştır.

1. Introduction

Ceramics developed to repair and reconstruct damaged or vestigial organs or to replace them, are called bioceramics. In general, calcium silicate-based materials are the candidate for bioceramic materials to be used for repair and regeneration of hard tissues due to their unique bioactivities [1-7]. Therefore, they find themselves a wide area of application in the health sector [8-10]. They also demonstrate anti-bacterial activity [11] and are used as insulation materials due to their fire-retardant characteristics [12]. The biocompatibility, thermal insulation ability and mechanical properties of them are determined by their crystalline structure, size, composition and morphology. Therefore, controlling the structural, physical and chemical properties of are of great importance in the industrial and biomedical applications. A literature studies indicate that the structural, physical and chemical properties of bioceramic materials are changed based on the synthesis method and the conditions [13-15]. Ceramic materials synthesized by sol-gel (SG) method have better chemical and structural homogeneity, and higher bioactivity, than those produced by other methods [16-18]. However, the synthesis of calcium silicate by SG method, using an acid or a base catalyst to accelerate the hydrolysis of tetraethyl orthosilicate (TEOS) is a disadvantage when considering and constructing a sustainable environmental awareness [11]. Over the last years, although the hydrothermal (HT) synthesis method has been successfully used for organic and inorganic syntheses [19], there are a few studies for synthesis of calcium silicate through an environmentally friendly and 'green synthesis HT method using water

* Corresponding author: ftomul@mehmetakif.edu.tr

instead of any organic solvents and auxiliary substances. Therefore, 'green' HT method for calcium silicate synthesis is of great significance based on environment and sustainable chemistry.

Thus, the purpose of this study is to produce new-generation calcium silicate material for biomedical and industrial applications through an easy, low-cost and environmentally friendly HT synthesis method using calcium nitrate and TEOS instead of any acids and organic solvents. SG synthesis method was also used for comparison. Fourier Transform Infrared Spectroscopy (FTIR), Thermogravimetric Analysis (TGA/DTA), Field Emission Scanning Electron Microscopy (FE-SEM), X-ray Diffraction (XRD) and Energy Dispersive Spectroscopy (EDS) methods were used to characterize calcium silicate bioceramic materials. Additionally, effects of the Ca/Si ratio and sintering temperature on the morphology and composition of calcium silicate materials were also investigated.

2. Material and Method

During synthesis, $Ca(NO_3)_2.4H_2O$ (calcium nitrate tetrahydrate, Sigma Aldrich) and $Si(OC_2H_5)_4$ (tetraethyl orthosilicate, TEOS, Sigma Aldrich), were used as calcium and silicon sources, respectively. Furthermore, HNO_3 (nitric acid, Merck) and C_2H_5OH (ethyl alcohol, Sigma Aldrich) were used as catalyst and solvent, respectively. All solutions were of analytical reagent grade and prepared using 18 MΩ.cm de-ionized water. Calcium silicate were synthesized using the method suggested by Chen et al [11].

2.1. Synthesis of calcium silicate by Hydrothermal (HT) method

In the first step, TEOS was added into water (1/10 ratio by volume) drop by drop and they were mixed for 2 hours and kept for a while. In the second step, sufficient amount of $Ca(NO_3)_2.4H_2O$ were added to above aqueous solution to obtain the desired Ca/Si ratio (0.67, 0.83, 1.0, 1.2 and 1.5) and then they were mixed to obtain a gel in ambient conditions at 24 h. The mixture was then put inside covered Teflon cups and kept in an oven at 120°C for one day for maturation of the gel and finally cooled until ambient temperature. Finally, cover was opened to remove water and any organic/inorganic solvents and kept at 120 °C for 24 h.

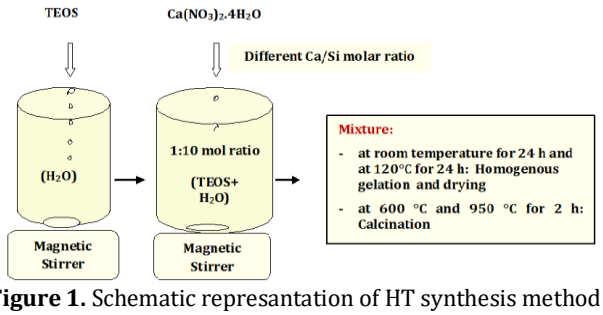

Figure 1. Schematic represantation of HT synthesis method

2.2. Synthesis of calcium silicate by Sol-Gel (SG) method

Fistly, HNO_3 and ethyl alcohol were added into TEOS solution as 10:10:1 molar ratio (HNO_3:ethyl alcohol:TEOS), respectively and they were mixed at 1 h. Secondly, sufficient $Ca(NO_3)_2.4H_2O$ was added on above solution to obtain the desired Ca/Si ratios (0.67, 1.0 and 1.5) and then mixed at 1 h. Finally, the solution was put into a polypropylene bottle with an impermeable cover at 60°C and kept in an oven for a day to obtain a gel.

The materials obtained by both methods were calcined at 600°C and 950°C at 10°C/min heating rate in an ash oven at 2 h to sinter them completely and to obtain the calcium silicate powder. The products were coded as 0.67Ca/Si-HT600 or 0.67Ca/Si-SG600 for specifying the ratio of Ca/Si, synthesis method and sintering temperature, respectively.

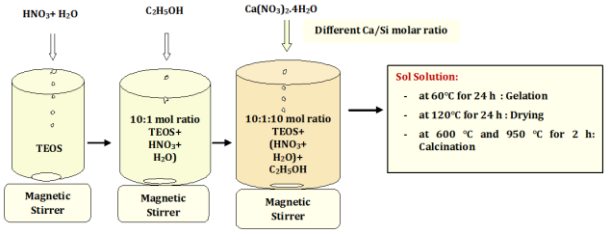

Figure 2. Schematic represantation of SG synthesis method

2.3. Characterization studies

XRD (A Bruker AXS D8 Advance Model powder diffractometer) with Cu-Kα radiation operated at 40 kV and 40 mA was used for the crystalline material measurements obtained from 10° to 70° at 1.2°/min rate and 0.02° step size. EDS (Bruker) was used to determine elemental compositions of materials. Additionally, morphologies of them were investigated by FE-SEM (ZEISS Supra 55). FTIR (Perkin Elmer) spectra of materials performed using the KBr pellet with a 4 cm^{-1} resolution in the range of between 4000 and 400 cm^{-1} were taken to determine the functional groups. TGA/DTA (Seiko SII TG 7200) measurements of materials using nitrogen gas at 10°C/min heating rate from ambient atmosphere to 1000°C were performed to determine their sintering reactions.

2.4. Bioactivity studies

Bioactivity studies of calcium silicate materials synthesized by HT and SG methods were performed in Simulated Body Fluid (SBF). It was prepared according to composition of blood, ion concentration and pH [20]. For this, 150 mg calcium silicate powder samples were pelleted under 3 MPa, then immersed in 30 mL of SBF in the polyethylene bottles and incubated for 7, 14, 28 and 34 days in a shaking water bath at 37 °C. During the waiting period, SBF was renewed as every 2 days to avoid the change for the

cation concentrations [21]. After reaching the desired retention times, the pellets were removed from the mixture by filtration, washed with de-ionized water and then dried in ambient conditions. The hydroxyapatite formation was investigated by XRD. Additionally, XRD was used to determine the phases formed in the materials suspended in SBF.

3. Results

3.1. XRD Patterns

XRD patterns of materials synthesized using the HT and SG methods with different Ca/Si ratios, and calcined at 600 °C and at 950 °C were shown in Figures 3 and 4, respectively.The sharp and strong peaks observed in the XRD patterns of materials synthesized by both methods indicate that calcium silicate materials were efficiently crystallized. On the other hand, for the material synthesized by HT method with a 0.67 Ca/Si and calcined at 600 °C for 2 h, the weak peaks were observed at 2θ = 32.43°. Additionally, peak at 41.06° indicated the formation of a larnite (β-Ca2SiO4) phase [1, 11, 22]. Weak peaks observed in the XRD pattern of the 0.67Ca/Si-HT600 material at 2θ = 37.26° and 53.77° were due to formation of a lime (CaO) compound. The weak magnitudes of peaks revealed that the amounts and crystallinity of the phases in this material were extremly low. On the other hand, it was observed that the magnitudes of peaks at 2θ = 32.43° and 41.06° due to a larnite phase, and at 2θ = 37.26° and 53.77° due to a lime phase were increased when Ca/Si ratio was increased and the highest peak magnitude was obtained in the case Ca/Si ratio was 1.5 (Figure 3A). These results showed that increasing calcium amount, and therefore the amount of crystallinity favored the formation of larnite and lime phases [11, 23].

After calcination of materials at 950 °C, peak at 2θ = 17.66° due to a portlandite phase [22], peaks at 2θ = 23.16°, 25.27°, 26.86° and 29.95° due to a wollastonite phase and a peak at 2θ = 29.3° due to a calcite phase were observed in the XRD patterns of 0.67Ca/Si-HT950 and 0.83Ca/Si-HT950 (Figure 3B). It was seen that a calcite phase observed at 2θ = 29.3° was not observed in other materials and the magnitudes of the peaks of the wollastonite phase at 2θ = 23.16°, 25.27°, 26.86° and 29.95° decreased with increasing Ca/Si ratio. Chen et al. [11] and Ciprioti et al. [23] observed the wollastonite phase in calcium silicate materials with a low amount of calcium. In general, calcium silicate based materials have been widely used in many industrial sectors due to their unique characteristics. Among them, the wollastonite has been preferred as a filler material in rubber, paper, ceramics and building sectors due to its moisture stability, air permeability, its fire-retardant, non-toxic characteristics, not dissolving in water and/or organic solvents, and its high hardness value [24, 25].

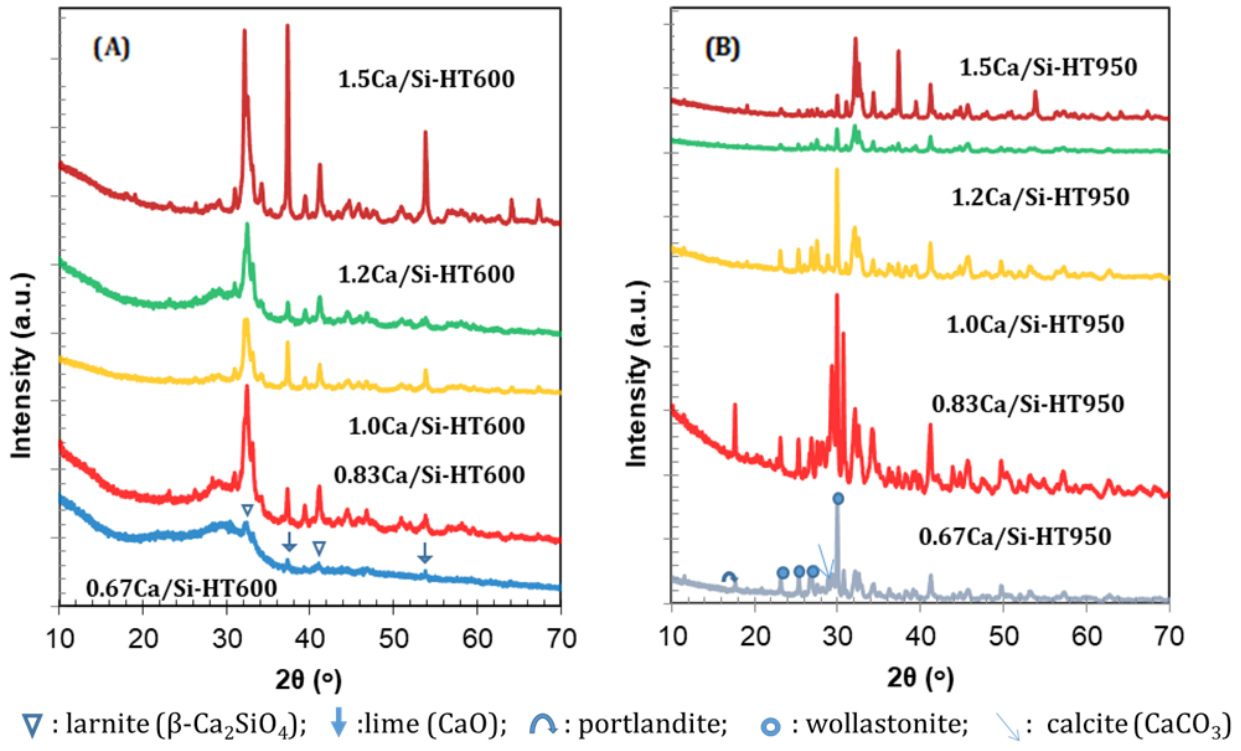

Figure 3. XRD patterns of calcium silicate bioceramic materials prepared by HT synthesis calcined at (A): 600°C (B): 950°C.

When the XRD patterns of materials (Ca/Si ratios were 0.67, 1.0 and 1.5, respectively) synthesized by SG method and calcined at 600 °C (Figure 4A) were

investigated, peaks at 2θ = 17.95° and 46.89° due to a portlandite phase and peak at 2θ=29.3° due to a calcite phase were present for material with a Ca/Si ratio of 0.67. It was seen that the portlandite phase disappeared in the product with a Ca/Si ratio of 1.0, while the magnitude of the peak belonging to the calcite phase observed at 2θ = 29.3° was increased. However, for the material with a Ca/Si ratio of 1.5, the magnitudes of peaks belonging to the portlandite and calcite phases were considerably increased. Moreover, for this material, new peaks due to a larnite phase were observed at 2θ = 33.14° and 33.94°, respectively [26]. When the effects of calcination temperature on crystalline structure of materials synthesized by SG method were investigated, peaks due to a portlandite phase (observed at 2θ = 17.9°) and a calcite phase (observed at 2θ = 29.3°) were disappeared for the 0.67Ca/Si-SG600 material in the case of increasing calcination temperature from 600°C to 950°C; however, a vaterite phase due to $CaCO_3$ was formed at 2θ = 27.51° [22]. In addition, new peaks due to wollastonite phase observed at 2θ = 23.13°, 25.28°, 25.97°, 26.87° and 29.95° (Figure 4B). It showed that the characteristic peaks of the larnite, calcite, lime and wollastonite phases were preserved when Ca/Si ratio was increased, but magnitude of peak belonging to the wollastonite phase was decreased as seen in materials synthesized by the HT method.

Phases observed in materials synthesized by both methods were consistent with those formed in materials synthesized by using the same, or different, silica and calcium sources and ratios in the literature. Baciu and Simitzis [27] reported that an amorphous glassy phase formed after calcination at 700 °C, and a $CaSiO_3$ crystal phase was formed after calcination at 1000 °C in the material synthesized by SG method using TEOS and $Ca(NO_3)_2$ in which Ca/Si ratio was 1.0. On the other hand, Chiang et al. [26] indicated that a β-$Ca2SiO_4$ phase was formed in the product calcined at 800 °C for 2 h in which Ca/Si ratio was 1.5 synthesized by the SG method.

3.2. FE-SEM-EDS analysis results

FE-SEM images of calcium silicate materials were obtained to determine their shape and surface structures. Additionally, their chemical compositions in the stack phase were investigated by EDS analysis. Elemental distribution maps of some materials were also produced to investigate distribution of elements. When FE-SEM images of calcium silicate materials calcined at 600 °C and 950 °C were investigated with a magnification of 100,000, it was seen that the surface structures of the materials synthesized by the HT method were changed with respect to Ca/Si ratio (Figure 5). A sponge-like morphology/structure consisting of spherical particles was observed in the materials in which Ca/Si ratios were 0.67, 0.83 and 1.0 calcined at 600 °C, while particles with various dimensions and shapes were formed in the materials in which Ca/Si ratio was higher than 1.0.

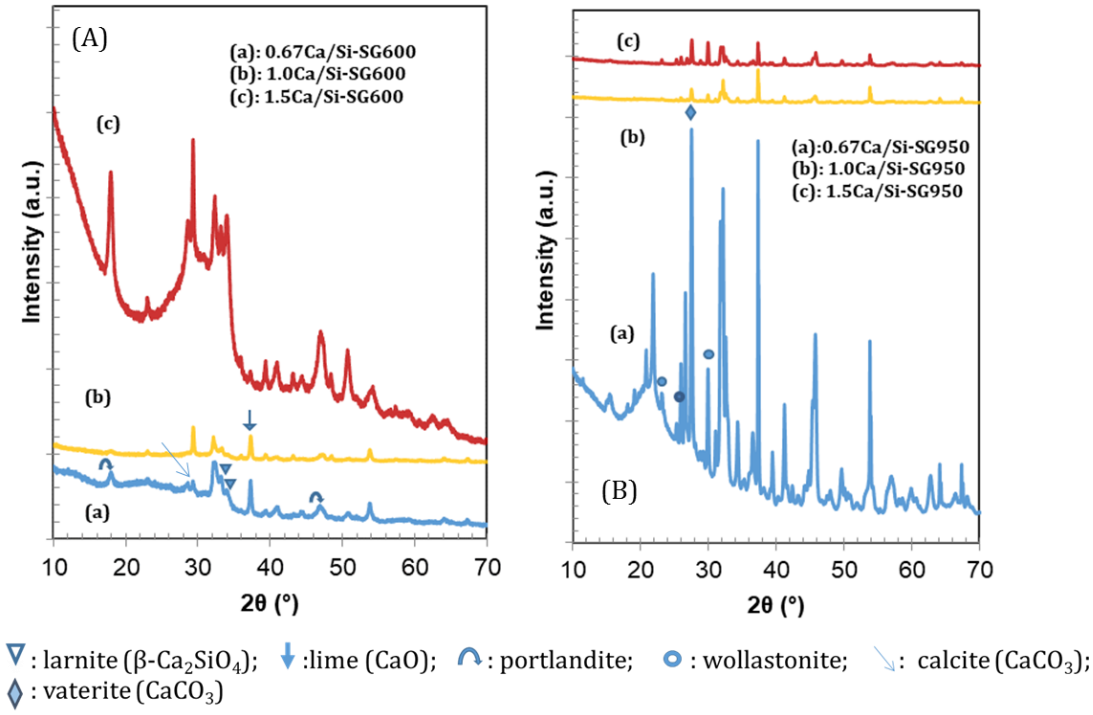

Figure 4. XRD patterns of calcium silicate bioceramic materials prepared by SG synthesis calcined at (A): 600°C (B): 950°C.

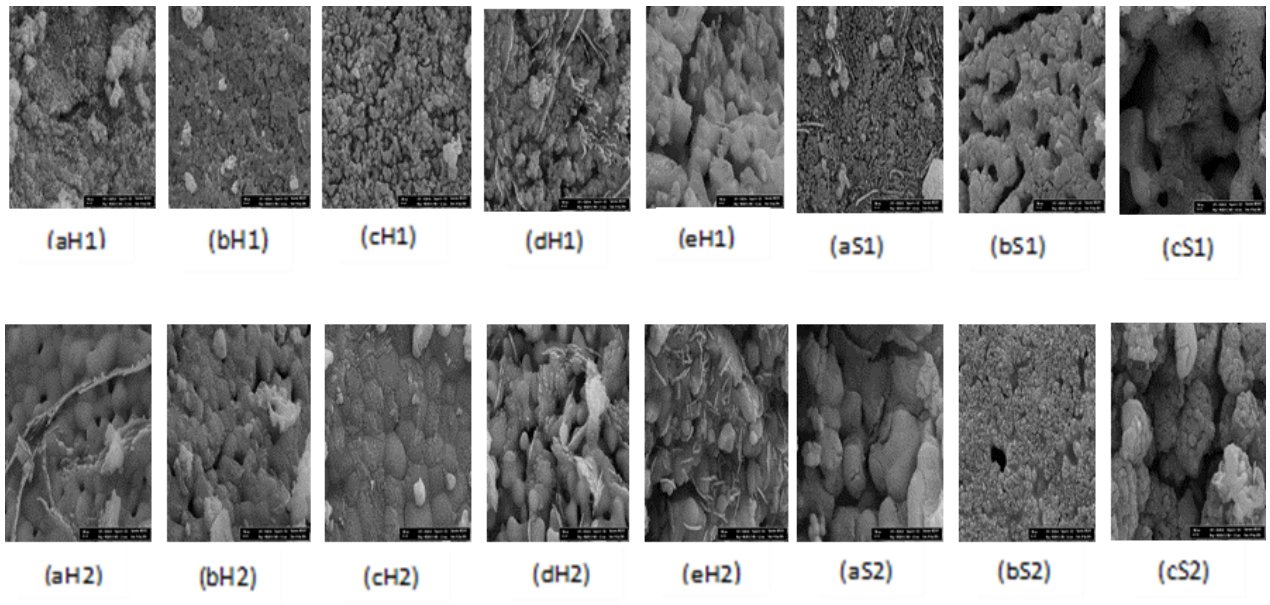

Figure 5. FE-SEM micrographs of calcium silicate bioceramics materials prepared by HT and SG synthesis methods as (aH1:0.67Ca/Si-HT600; bH1:0.83Ca/Si-HT600; cH1:1.0Ca/Si-HT600; dH1:1.2Ca/Si-HT600; eH1:1.5Ca/Si-HT600; aS1:0.67Ca/Si-SG600: bS1:1.0Ca/Si-SG600; cS1:1.5Ca/Si-SG600; aH2:0.67Ca/Si-HT950; bH2:0.83Ca/Si-HT950; cH2:1.0Ca/Si-HT950; dH2:1.2Ca/Si-HT950; eH2:1.5Ca/Si-HT950; aS2:0.67Ca/Si-SG950: bS2:1.0Ca/Si-SG950; cS2:1.5Ca/Si-SG950

Additionally, it was observed that gaps between grains were increased. Particularly in the materials in which a Ca/Si ratio was 1.2, a structure consisting of a laminated leaf and fibers of various lengths was formed. In materials where a Ca/Si ratio was lower than 1.0, although gaps were formed between the particles due to increasing calcination temperature from 600 °C to 950 °C, it was seen that the particles were bonded more tightly to each other. On the other hand, in the products in which a Ca/Si ratio was higher than 1.0, it was observed that both particle and pore sizes were increased in the case calcination temperature was increased to 950 °C. Moreover, cracks were formed on the surfaces of materials depending on the removal of gases formed due to the increase in calcination temperature. It was also observed that due to agglomeration of small-sized particles, large-sized particles were formed as a result of the increasing temperature. It was observed that the surface morphologies of the materials synthesized by SG method similar to the HT synthesis method but they were changed with respect to the Ca/Si ratio. However, more homogeneous particles were obtained in SG synthesis method compared to the particles synthesized by the HT method and higher amounts of cracks were formed on the surfaces of particles depending on the removal of gases formed due to heating, and higher amounts of gaps were present between particles. The fibrous structure observed in the material synthesized by HT method and calcined at 600 °C in which a Ca/Si ratio was 1.2 was also observed in the material in which a Ca/Si ratio was 0.67 synthesized by SG method and calcined at 600 °C. These results revealed that both synthesis method and ratio of Ca/Si influenced morphologies of calcium silicate materials.

EDS analyses of materials where Ca/Si ratios were 0.67, 1.0 and 1.5, respectively synthesized by HT and SG methods, were also performed and the amounts of calcium and silicon were summarized in Table 1 as calcium oxide (CaO) and silicon dioxide (SiO_2), respectively.

Table 1. CaO and SiO_2 percentages of calcium silicate bioceramic materials, which are obtained by energy dispersive spectroscopy (EDS)

Samples prepared by using HT synthesis method					
Sample code	CaO (%)	SiO_2 (%)	Sample code	CaO (%)	SiO_2 (%)
0.67Ca/Si-HT600	35.47	64.53	0.67Ca/Si-HT950	34.33	65.67
0.83Ca/Si- HT600	48.69	51.31	0.83Ca/Si- HT950	45.72	54.28
1.0Ca/Si- HT600	60.78	39.22	1.0Ca/Si- HT950	56.73	43.27
1.2Ca/Si- HT600	63.85	36.15	1.2Ca/Si- HT950	63.47	36.53
1.5Ca/Si- HT600	72.59	27.41	1.5Ca/Si- HT950	69.42	30.58
Samples prepared by using SG synthesis method					
0.67Ca/Si-SG600	17.84	82.16	0.67Ca/Si-SG950	15.68	84.32
1.0Ca/Si- SG600	54.83	45.17	1.0Ca/Si- SG950	52.82	47.18
1.5Ca/Si- SG600	56.56	43.44	1.5Ca/Si- SG950	55.42	44.58

It was observed that the amounts of CaO and SiO_2 in the materials were changed with respect to the synthesis method and sintering temperature. CaO/SiO_2 ratios obtained from the EDS analyses did not equal the theoretical Ca/Si ratios. Ca was lower than the theoretical value in materials having a lower Ca content, while it was higher than the theoretical value in materials having a higher Ca content. This phenomenon could be explained by the decrease in silicon hydrolysis with increasing Ca content under HT synthesis conditions. By contrast, while Ca/Si ratio was higher than the theoretical one for materials synthesized by SG method in which Ca/Si ratio was 1.0, that was lower in other materials. This result could be due to the fact that the effects of the increase in the Ca amount on silicon hydrolysis in SG synthesis conditions were less in the HT method.

Figure 6 showed elemental distribution maps of the materials in which a Ca/Si ratio was 1.5 synthesized by the HT method and calcined from 600 °C to 950 °C, as well as the material having the same Ca/Si ratio but synthesized by SG method and calcined at 600 °C. It was observed that Ca, Si and O elements were present at different concentrations and they were concentrated in certain regions.

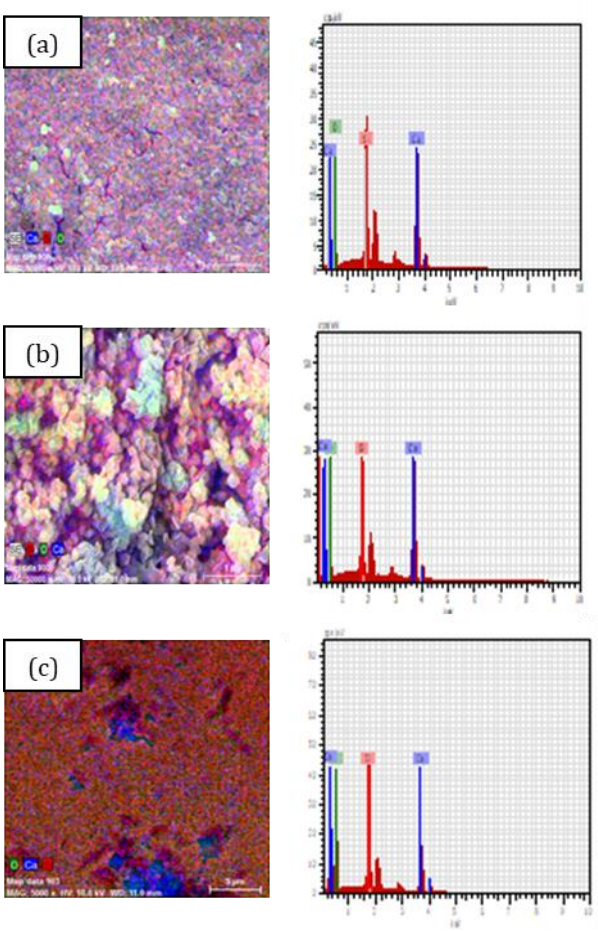

Figure 6. EDS mapping analysis of (a) 1.5 Ca/Si-HT600 sample (b) 1.5 Ca/Si-HT950 and (c) 1.5 Ca/Si-SG600 samples

3.3. FTIR spectra of samples

FTIR spectra of calcium silicate materials synthesized by HT and SG methods, and calcined at different temperatures were shown in Figure 7 and Figure 8, respectively. In the material in which a Ca/Si ratio was 0.67 and calcined at 600 °C, characteristic bands were observed at 470 cm^{-1}, 490 cm^{-1} and 668 cm^{-1}, indicating bending vibration of Si-O-Si bonds in the SiO_4 tetrahedron. Moreover, in the same material, a broad peak was observed at 1035 cm^{-1} due to stretching vibration of the Si-O-Si bonds in the SiO_4 tetrahedron. A broad and weak peak was observed between 1335 cm^{-1} to 1556 cm^{-1} for a carbonate group [28, 29]. Although for the material where a Ca/Si ratio was 0.67 and calcined at 600°C, peak was observed at 1035 cm^{-1} due to Si-O-Si stretching, when increasing the Ca/Si ratio, peaks were divided into three at 996 cm^{-1}, 921 cm^{-1} and 848 cm^{-1} due to forming Si-O-Ca bonds [30, 31], and the highest magnitude peaks were obtained for the material in which a Ca/Si ratio was 1.5. Moreover, in the material having the highest calcium content, a strong peak, different from other materials, was observed 518 cm^{-1} due to the Si-O-Ca bond (Figure 7A). Peaks observed at 921 cm^{-1} and 518 cm^{-1} indicated the larnite crystalline phase, while the peak observed at 848 cm^{-1} indicated the wollastonite crystalline phase [28]. Changes observed in FTIR spectra were due to transformations caused by diffusing calcium ions into the Si-O-Si network. The FTIR results validated the XRD results. FTIR spectra and the peak positions due to the stretching and bending vibrations of Si-O-Si bonds for calcium silicate materials were consistent with Wang et al. [22] and Ciprioti et al. [23].

FTIR spectra of materials synthesized by the HT method and calcined at 950 °C were shown in Figure 7B. For materials in which a Ca/Si ratio was higher than 0.67 and calcined at 600 °C, a division was observed in the peaks between 800 cm^{-1} and 1200 cm^{-1} due to increasing calcination temperature. Moreover, it was observed that the magnitude of the divided peaks was higher than those materials calcined at 600 °C. On the other hand, after calcination at 950 °C, the presence of peaks at 650 cm^{-1} and 750 cm^{-1} due to $CaSiO_3$ was obtained for all materials except for those materials in which Ca/Si ratios were 0.67 and 1.5, respectively. Moreover, carbonate peaks observed between 1335 cm^{-1} and 1556 cm^{-1}, due to increasing calcination temperature, were not seen in the materials having a low Ca/Si ratio. Changes observed in FTIR spectra based on increasing calcination temperature revealed that transformations formed in the Si-O-Si network due to the temperature effect.

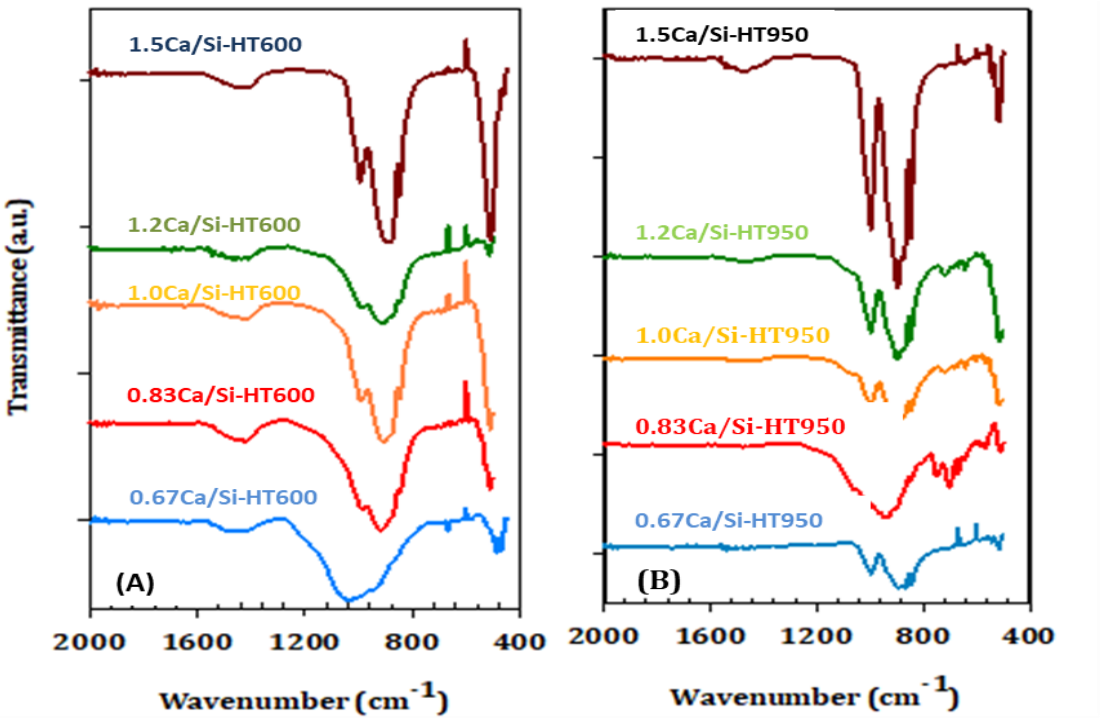

Figure 7. FTIR spectra of calcium silicate bioceramic materials prepared by HT synthesis calcined at (A): 600°C (B): 950°C

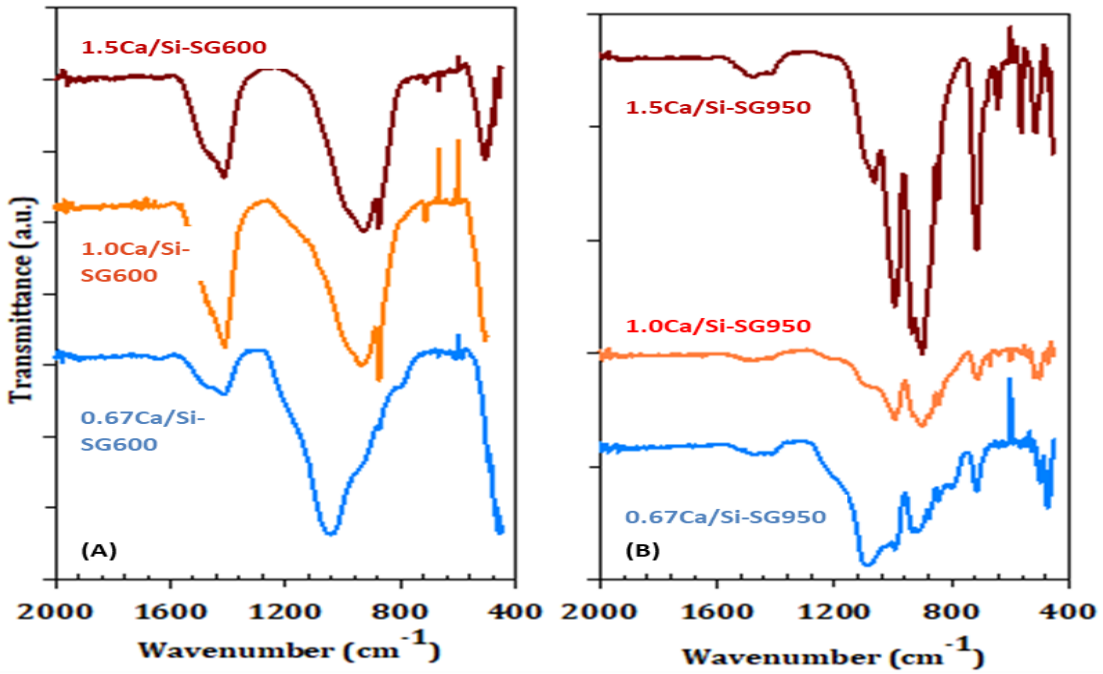

Figure 8. FTIR spectra of calcium silicate bioceramic materials prepared by SG method calcined at (A): 600°C (B): 950°C

By contrast, FTIR spectra of materials synthesized by SG method and calcined at different temperatures were different from that of materials synthesized by the HT method. It was seen that for the material in which a Ca/Si ratio was 0.67 and calcined at 600 °C, a broad peak was observed at 1035 cm^{-1}. Due to an increasing Ca/Si ratio, that was divided into two peaks at 937 cm^{-1} and 875 cm^{-1} and the magnitudes of the broad and weak peaks for characteristic band of carbonate group between 1335 cm^{-1} and 1556 cm^{-1} were considerably increased (Figure 8A). As a result of increasing calcination temperature, many new peaks formed in three materials between 400 and 1000 cm^{-1} due to Si-O-Si stretching and bending vibrations, and formation of the Si-O-Ca bond. It was observed that magnitudes of some newly formed peaks were at maximum in the materials having the highest Ca/Si ratio (Figure 8B).

3.4. TG/DTA analyses

Simultaneous TG/DTA analyses were performed for different temperature from ambient atmosphere to 1000 °C to investigate the thermal behaviours of materials in which a Ca/Si ratio was 1.5 and calcined at 950 °C synthesized by the HT method and dried at 120 °C. TG/DTA analyses were also performed in the same temperature range to to investigate the effects of the synthesis method on the thermal behaviour of the materials by SG method. The results were shown in Figure 9. The mass losses were observed after stepwise reactions. It was observed in Figure 9 that the mass loss was continuously proceeded with increased heating rate, and it was continued from ambient atmosphere to 1000°C with increasing and decreasing rates.

The mass loss of the material where a Ca/Si ratio was 0.67 was found to be approximately 53%. It was sometimes proceeded rapidly and sometimes proceeded slowly, and stopped in some regions; but it could be understood that it was proceeded dynamically from ambient atmosphere to 1000°C. Approximately 36% mass loss was occurred in a temperature range from 500 to 600 °C and 69% of the total mass loss was occurred at this time. Approximately 12% of the mass loss was occurred up to 500 °C. This percentage was constituting about 23% of the total mass loss. The increases in total mass losses were observed with increasing Ca/Si ratio. Maximum temperatures of apparent endothermic peaks observed in the DTA curve of the material in which a Ca/Si ratio was 0.67 were found to be 108 °C and 547 °C, respectively, while the temperature of a single exothermic peak was found to be 872 °C (Figure 9B). The first endothermic peak showed the withdrawal of physical water from the structure [32], while the second one indicated temperature transitions accompanying the degradation of organics/nitrates [33]. It was considered that the exothermic peak was due to the formation of crystalline structures from the amorphous state or transformations/oxidations in the crystalline state. Increases in crystallinity of this product that were seen in XRD patterns after calcination at 950 °C supported this result. Increases in the number of endothermic peaks observed below 200 °C, due to increases in the Ca/Si ratio, indicated that the withdrawal of physical water was occurred in two or three steps with respect to the number of peaks formed, while increases observed above 500 °C revealed that organics/nitrates were removed in a few steps. When TG/DTA curves of the material synthesized by the HT synthesis method in which a Ca/Si ratio was 1.5 and were compared to the material with same Ca/Si ratio but synthesized by SG method, it was observed that their total mass losses were close to each other, but their mass loss tendencies were opposite. Although the highest mass loss in the material synthesized by HT was observed in a temperature range from 500 to 600 °C, the highest mass loss in the material synthesized by SG was observed in the region of 500 °C, resulting in 85% of the total mass loss.

3.5. Evaluation of in vitro bioactivity results

XRD patterns of the materials incubated in SBF at 37 ° C for 7, 14, 28 and 34 days were shown in Figure 10, respectively. The ability of calcium silicate materials with different Ca/Si ratio to form hydroxy apatite was depending on the Ca/Si ratio. Since the presence of intense peaks were observed at about 2θ = 26 ° and 32° due to hydroxy apatite in the case Ca/Si ratios were 0.67 and 1.5, the lowest and highest calcium silicate materials had a better ability to form hydroxyapatite than the other materials. The formation of hydroxy apatite was observed after 28th days in the material including low calcium content (0.67Ca/Si-HT-950), whereas it was observed after 7th days in the material including high calcium content (1.5Ca/Si-HT-950).

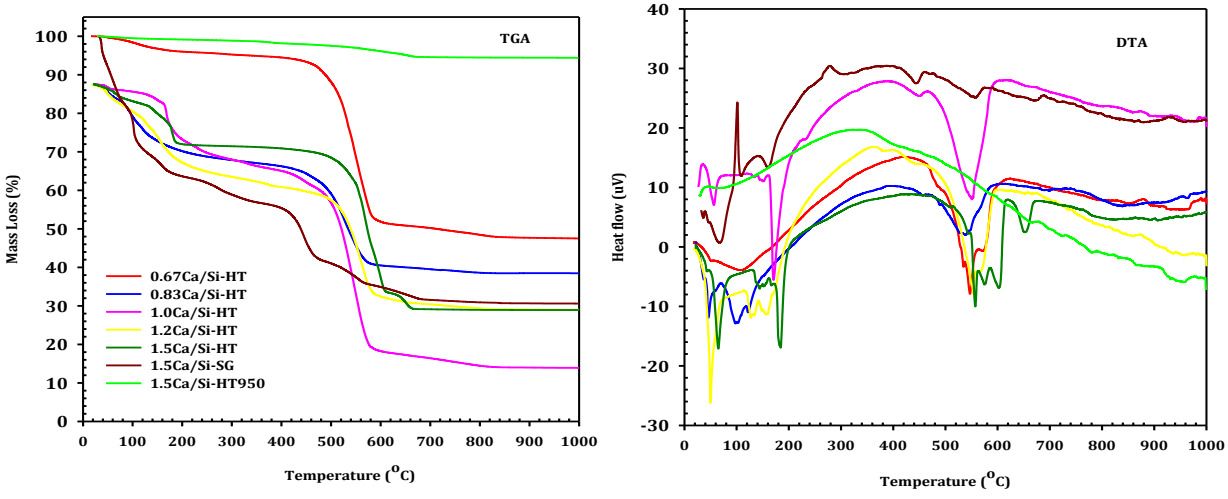

Figure 9. TG/DTA curve of of calcium silicate bioceramic materials prepared by HT and SG synthesis

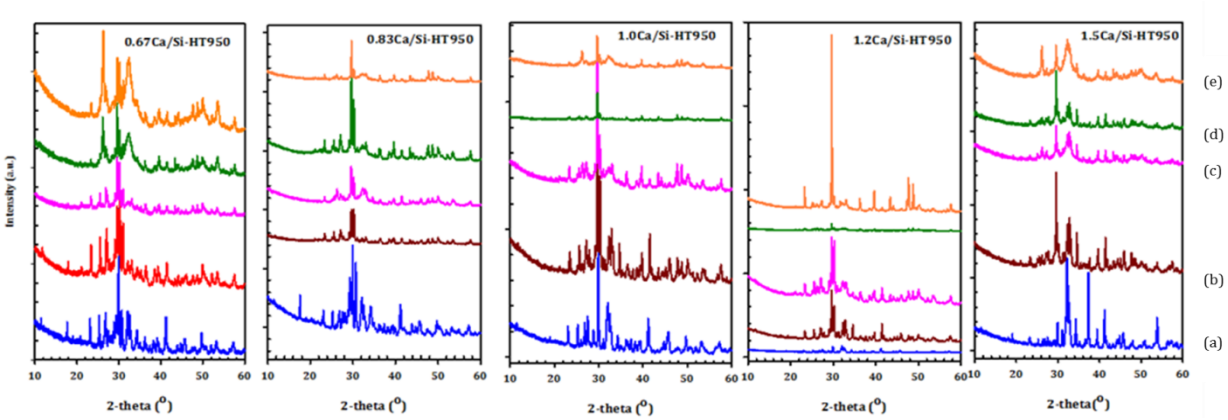

Figure 10. XRD patterns of materials prepared HT synthesis method calcined at 950°C. (a) no treatment with SBF (b)7 days (c) 14 days (d) 28 and (e) 34 days treatment with SBF, respectively

4. Discussion and Conclusion

In this study calcium silicate bioceramic materials were synthesized by HT and SG methods, respectively. Furthermore, the properties of the synthesized materials are satisfactory for the biomedical applications. The mechanism of the synthesis of the calcium silicate bioceramic materials are based on inorganic polymerization reactions including metal alkoxide precursors. The hydrolysis and condensation of these precursors cause to form calcium silicate bioceramic materials [27].

As a result of mineralogical analyses performed by the X-ray diffraction method, larnite and lime phases were observed in all materials prepared by the HT synthesis method and calcined at 600 °C, and it was seen that the magnitudes of these phases increased with increasing Ca/Si ratio. After calcination at 950 °C, the presence of portlandite, wollastonite and calcite phases, in addition to larnite and lime phases, was also observed. It was seen that the magnitude of the peak belonging to the wollastonite phase decreased with increasing Ca/Si ratio. However, portlandite and calcite phases were observed with larnite and lime phases in the material in which a Ca/Si ratio was 0.67 synthesized by SG method and calcined at 600 °C, unlike the material synthesized by the HT method. Significant differences were observed in SEM images of calcium silicate materials having different Ca/Si ratios, in accordance with XRD results, depending on the synthesis method and the calcination temperature. The morphology of the material changed from cubic shaped to laminated leaf and fibers with various lengths, depending on the Ca/Si ratio increase. EDS analysis results did not validate theoretical Ca/Si ratios. It could be seen from TG/DTA analysis results that the most important mass losses were in temperature from 500 to 600 °C. The highest and lowest mass losses in this temperature range were obtained for 1.0Ca/Si-HT and 0.67Ca/Si-HT materials, respectively. It was determined that the mass loss was observed in the material where a Ca/Si ratio was 1.5 synthesized by SG method (1.5Ca/Si-SG) was higher than that synthesized by the HT method (1.5Ca/Si-HT). It was determined that the mass loss of the material calcined at 950°C was low.

The main novelty of this study is that calcium silicate bioceramic materials were synthesized at ambient temperature and pressure and the synthesis was performed in only water without need any acids or bases. Additionally, the properties of materials obtained by HT synthesis are comparable with that of SG method. Therefore, because any chemical products and hazardous substances were not used, synthesis conditions refer the green chemistry.

Acknowledgements

The Scientific and Technical Research Council of Turkey (TÜBİTAK/BİDEP 2209A, Reference Number: 1919B011501496) supported this study.

References

[1] Ho, C.-C., Wei, C.-K., Lin, S.-Y., Ding, S.-J. 2016. Calcium silicate cements prepared by hydrothermal synthesis for bone repair. Ceram. Int., 42, 9183-9189.

[2] Niu, L., Jiao, K., Wang, T., Zhang, W., Camilleri, J., Bergeron, B.-E., Feng, H., Mao, J., Chen, J., Pashley, D.-H., Tay, F.-R. 2014. A review of the bioactivity of hydraulic calcium silicate cements. J. Dentistry., 42, 517-533.

[3] Sun, Y.-S., Li, A.-L., Renb, H.-H., Zhang, X.-P., Wang, C., Qiu, D. 2016 Removal of residual nitrate ion from bioactive calcium silicate through soaking. Chin. Chem. Lett., 27, 579–582.

[4] Ding, S.-J., Shie, M.-Y., Wei, C.-K. 2011. In vitro physicochemical properties, osteogenic activity, and immunocompatibility of calcium silicate–gelatin bone grafts for load-bearing applications. ACS Appl Mater Interfaces., 3, 4142-4153.

[5] Giannoulatou, V., Theodorou, G.-S., Zorba, T., Kontonasaki, E., Papadopoulou, L., Kantiranis, N., Paraskevopoulos, K.-M. 2018. Magnesium calcium silicate bioactive glass doped with

copper ions; synthesis and in-vitro bioactivity characterization. Journal of Non-Crystalline Solids, 500, 98-109.

[6] Chen, L., Deng, C., Li, J., Yao, Q., Chang, J., Wang, L., Wu, C. 2019. 3D printing of a lithium-calcium-silicate crystal bioscaffold with dual bioactivities for osteochondral interface reconstruction. Biomaterials, 196, 138-150.

[7] Zhang, Q., Chen, L., Chen, B., Chen, C., Chang, J., Xiao, Y., Yan, F. 2019. Lithium-calcium-silicate bioceramics stimulating cementogenic/ osteogenic differentiation of periodontal ligament cells and periodontal regeneration. Applied Materials Today, 16, 375-387.

[8] Liu, C.-H., Hung, C.J., Huang, T.H., Lin, C.C., Kao, C.T., Shie, M.Y. 2014. Odontogenic differentiation of human dental pulp cells by calcium silicate materials stimulating via FGFR/ERK signaling pathway, Materials Science and Engineering: C, 43, 359-366.

[9] Lu, B.Q., Zhu, Y.J., Ao, H.Y., Qi, C., Chen, F. 2012. Synthesis and Characterization of Magnetic Iron Oxide/Calcium Silicate Mesoporous Nanocomposites as a Promising Vehicle for Drug Delivery, ACS Applied Materials Interfaces, 4, 6969−6974.

[10] Shirazi, F.S., Mehrali, M., Oshkour, A.A., Metselaar, H.S.C., Kadri, N.A., Osman, N.A.A. 2014. Mechanical and physical properties of calcium silicate/alumina composite for biomedical engineering applications, Journal of the Mechanical Behavior of Biomedical Materials, 30, 168-175.

[11] Chen, C.C., Ho, C.-C., Lin, S.Y., Ding, S.J. 2015. Green synthesis of calcium silicate bioceramic powders, Ceram. Int., 41, 5445–5453.

[12] Li, M., Liang, H. 2004. Formation of micro-porous spherical particles of calcium silicate (xonotlite) in dynamic hydrothermal process. China Particuology, 2, 124-127.

[13] Mehrali, M. Shirazi, S.-F.-S. Baradaran, S.; Mehrali, M.; Metselaar, H.-S.-C.; Bin Kadri, N.-A.;Osman, N.-A.-A. 2014. Facile synthesis of calcium silicate hydrate using sodium dodecyl sulfate as a surfactant assisted by ultrasonic irradiation. Ultrason. Sonochem. 21, 735–742.

[14] Roosz, C., Gaboreau, S., Grangeon, S., Prêt, D., Montouillout, V., Maubec, N., Ory, S., Blanc, P., Vieillard, P., Henocq, P. 2016. Distribution of water in synthetic calcium silicate hydrates. Langmuir. 32, 6794–6805.

[15] Yongjia, H., Xiaogang, Z., Linnu, L., Leslie, S., Shuguang, H. 2011. Effect of C/S Ratio on Morphology and Structure of Hydrothermally Synthesized Calcium Silicate Hydrate. J Wuhan Univ. Technol., 26, 770-773.

[16] Hench, L.-L., West, J.-K. 1990. The sol-gel process. Chem. Rev., 90, 33-72.

[17] Li, P., De Groot, K. 1994. Better bioactive ceramics through sol-gel process. J. Sol-Gel Sci. Technol., 2, 797-806.

[18] Meisztерics, A., Sinkó, K. 2008. Sol-gel derived calcium silicate seramics. Colloids Surf. A Physicochem. Eng. Asp., 319, 143-148.

[19] Zhang, N., Liu, W., Zhu, H., Chen, L., Lin, K., Chang, J. 2014. Tailoring Si-substitution level of Si-hydroxy apatite nanowires via regulating Si content of calcium silicates as hydrothermal precursors. Ceram. Int., 40, 11239-11243.

[20] Tas, A. -C. 2000. Synthesis of biomimetic Ca-hydroxyapatite powders at 37 C in synthetic body fluids. Biomaterials, 21, 1429-1438.

[21] Lakshmi, R., Sasikumar, S. 2015. Influence of needle-like morphology on the bioactivity of nanocrystalline wollastonite–an in vitro study. Int. J. Nanomedicine., 10, 129-136.

[22] Wang, F., Xu, Z., Zhang, Y., Li, J., Nian, S., Zhou, N. 2016. Green synthesis and bioactivity of vaterite-doped beta-dicalcium silicate bone cement. Ceram. Int., 42, 1856-1861.

[23] Ciprioti, S.-V., Catauro, M. 2016. Synthesis, structural and thermal behavior study of four Ca-containing silicate gel-glasses. J. Therm. Anal. Calorim., 123, 2091–2101.

[24] Akat'eva, L.-V., Gladun, V.-D., Khol'kin, A.-I. 2011. Use of Extractants in the Synthesis of Calcium Silicates and Calcium Silicate–Based Materials. Theor. Found. Chem. Eng., 45, 702–712.

[25] Lin, K., Chang, J., Chen, G., Ruan, M., Ning, C. 2007. A simple method to synthesize single-crystalline β-wollastonite nanowires. J. Cryst. Growth. 300, 267-271.

[26] Chiang, T.-Y., Wei, C.-K., Ding, S.-J. 2013. Effects of Bismuth Oxide on Physicochemical Propertiesand Osteogenic Activity of Dicalcium Silicate Cements. J. Med. Biol. Eng., 34, 30-35.

[27] Baciu, D., Simitzis, J. 2007. Synthesis and characterization of a calcium silicate bioactive glass. Optoelectron. Adv. Mat., 9, 3320-3324.

[28] Meisztерics, A., Rosta, L., Peterlik, H., Rohonczy, J., Kubuki, S., Henits, P., Sinkó, K. 2010. Structural characterization of gel-derived calcium silicate systems. J. Phys. Chem. A., 114, 10403-10411.

[29] Lee, Y.-L., Wang, W.-H., Lin, F.-H., Lin, C.-P. 2017. Hydration behaviors of calcium silicate-based biomaterials. J. Formos. Med. Assoc., 116, 424-431.

[30] Lakshmi, R., Sasikumar, S. 2015. Influence of needle-like morphology on the bioactivity of nanocrystalline wollastonite–an in vitro study. Int. J Nanomedicine., 10, 129-136.

[31] Padilla, S., Roman, J., Carenas, A., Vallet-Regi, M. 2005. The influence of the phosphorus content on the bioactivity of sol–gel glass ceramics. Biomaterials., 26, 475-483.

[32] Foley, E.-M., Kim, J.-J., Taha, M.-R. 2012. Synthesis and nano-mechanical characterization of calcium-silicate-hydrate (CSH) made with 1.5 CaO/SiO_2 mixture. Cem. Concr. Res., 42, 1225-1232.

[33] Sun, Y.-S., Li, A.-L., Xu, F.-J., Qiu, D. 2013. A low-temperature sol–gel route for the synthesis of bioactive calcium silicates. Chin. Chem. Lett., 24, 170–172.